Published in *Phys. Med. Biol.* **49**, 4407-4425 (2004).

Nonlinear cardio-respiratory interactions revealed by time-phase bispectral analysis

Janez Jamšek†‡§, Aneta Stefanovska†§ and Peter V E McClintock§‖

† Group of Nonlinear Dynamics and Synergetics, Faculty of Electrical Engineering, University of Ljubljana, Tržaška 25, 1000 Ljubljana, Slovenia.
‡ Department of Physics and Technical Studies, Faculty of Education, University of Ljubljana, Kardeljeva ploščad 16, 1000 Ljubljana, Slovenia.
§ Department of Physics, University of Lancaster, Lancaster LA1 4YB, UK.

PACS numbers: 02.70.Hm, 05.45.Xt, 05.40.-a

Abstract. Bispectral analysis based on high order statistics, introduced recently as a technique for revealing time-phase relationships among interacting noisy oscillators, has been used to study the nature of the coupling between cardiac and respiratory activity. Univariate blood flow signals recorded simultaneously by laser-Doppler flowmetry on both legs and arms were analysed. Coupling between cardiac and respiratory activity was also checked by use of bivariate data and computation of the cross-bispectrum between the ECG and respiratory signals. Measurements were made on six healthy males aged 25–27 years. Recordings were taken during spontaneous breathing (20 min), and during paced respiration at frequencies both lower and higher than that of spontaneous respiration (either two or three recordings with a constant frequency in the interval between 0.09 and 0.35 Hz). At each paced frequency recordings were taken for 12 min. It was confirmed that the dynamics of blood flow can usefully be considered in terms of coupled oscillators, and demonstrated that interactions between the cardiac and respiratory processes are weak and time-varying, and that they can be nonlinear. Nonlinear coupling was revealed to exist during both spontaneous and paced respiration. When present, it was detected in all four blood flow signals and in the cross-bispectrum between the ECG and respiratory signal. The episodes with nonlinear coupling were detected in 11 out of 22 recordings and lasted between 19 s in the case of high frequency (0.34 Hz) and 106 s in the case of low frequency paced respiration (0.11 Hz).

Submitted to: *Phys. Med. Biol.*

1. Introduction

It has long been known that the heart of a healthy human subject in repose does not beat regularly. The rhythmic variation in the heart rate occurring at the frequency of respiration is known as sinus respiratory arrhythmia (see e.g. Stefanovska (2002) or Eckberg (2003) and references therein); it is not the only source of arrythmia (Stefanovska and Bračič 1999). In fact, at least *five* characteristic frequencies can be

‖ To whom correspondence should be addressed (p.v.e.mcclintock@lancaster.ac.uk)

seen in blood flow signals, at ∼1 Hz, 0.3 Hz, 0.1 Hz, 0.04 Hz and 0.01 Hz. The first two components correspond to the cardiac and respiratory oscillators respectively. The component at ∼0.1 Hz is often attributed to intrinsic myogenic activity. The other two correspond respectively to neurogenic and endothelial related metabolic activity. The wavelet transforms of such signals have been discussed in detail (Bračič and Stefanovska 1998, Stefanovska *et al.* 1999, Bračič and Stefanovska 1999).

The cardiac and respiratory systems can be perceived from the nonlinear dynamics point of view as coupled autonomous oscillators, each with its own characteristic frequency (Stefanovska and Bračič 1999, Stefanovska *et al.* 2001a). It is respiratory sinus arrhythmia – the rhythmic fluctuations of electrocardiographic R-R intervals, or the rhythmic modulation of the instantaneous cardiac frequency – that provides the most obvious manifestation of their coupling. Although the interaction between the cardiac and respiratory rhythms has been known to exist since the early works by Hales (1773) and Ludwig (1847), the underlying physiological mechanisms are not completely understood. In his recent review Eckberg (2003) discusses several possible mechanisms for respiratory gating, of both central and peripheral origin: central, secondary to efferent respiratory motoneurone activity; and peripheral, secondary to afferent neural activity from pulmonary and thoracic stretch receptors. He presents a wide range of evidence favoring the influence of respiration on R-R interval fluctuations (as well as on the fluctuations in systolic blood pressure that are strongly correlated to the R-R fluctuations), rather than the influence of peripheral baroreceptor physiology as an origin of modulation. As the physiological mechanisms of cardio-respiratory coupling are not fully understood, even less is known about the nature of this coupling, e.g. whether it is linear, quadratic or even of higher order.

In addition to the modulation, a mutual adjustment of the cardiac and respiratory rhythms may occur, leading to their synchronization: in a conscious healthy subject at rest, the cardiac and respiratory systems have been shown to synchronize for short periods of time (Schäfer *et al.* 1998, 1999, Bračič Lotrič and Stefanovska 2000). The state of the system is characterized by the interactions and couplings between the oscillatory physiological processes. For instance, in anaesthesia the cardiac and respiratory systems synchronize for more extended periods of time (Stefanovska *et al.* 2000). A long-term aim is therefore to develop a coupled oscillator model that can provide a description of the system, quantifying the couplings and relating their values to its different states of health or disease. We may thus aim for improved techniques of early diagnosis, better assessment of the efficacy of treatment for a range of cardiovascular diseases, and perhaps quantification of depth of anæsthesia.

The interactions can be detected by analysis of recorded time series, and their strength and direction can also be determined (Schreiber 2000, Rosenblum and Pikovsky 2001, Paluš *et al.* 2001, Rosenblum *et al.* 2002, Paluš and Stefanovska 2003). The next logical step in studying interactions among the coupled oscillators must be to determine the nature of the couplings from the time series.

Jamšek *et al.* (2003) succeeded in extending bispectral analysis to encompass time dependence, and demonstrated the potential of the extended technique to determine the type of couplings among interacting nonlinear oscillators. Time-phase couplings can be observed by calculating the bispectrum and adapted bispectrum, thereby obtaining the time-dependent biphase and biamplitude. The method has the advantage that it allows an arbitrary number of interacting oscillatory processes to be studied. It is applicable both to univariate data (a single signal from the coupled system), and to multivariate data (a separate signal from each oscillator).

In the present paper, we apply the new technique to univariate cardiovascular (CV) blood flow signals that reflect the activities of both the local and central mechanisms of cardiovascular regulation. The heart's pumping action is manifested in every vessel, including the microcirculation. Peripheral blood flow is controlled by both extrinsic (central) and intrinsic (local) mechanisms, and so must reflect the activities of both the local and central regulatory mechanisms (Stefanovska and Bračič 1999, Stefanovska *et al.* 1999, Bračič *et al.* 2000, Söderström *et al.* 2003). In section 2 we summarize how measurements are made and discuss how the resultant data are analyzed. Results are presented in section 3, and are discussed in section 4, where it is shown that the cardiac and respiratory processes can be nonlinearly phase coupled. Finally, in section 5, the work is summarized and conclusions are drawn. Details of the normalization techniques used for comparison of the different measurements are given in Appendix A, and an analysis of harmonic generation by a pair of weakly-coupled weakly-nonlinear oscillators is presented in Appendix B.

2. Data acquisition and analysis techniques

The interaction between two harmonic components can in practice contribute to the power at their sum and/or difference frequencies. We assume that the cardiac and respiratory oscillators are weakly coupled and can interact with each other nonlinearly. The coupling is assumed to be weak in part because of the transient/episodic character of cardio-respiratory synchronization in healthy subjects; the assumption of weak nonlinearity is on account of several factors including the lack of combinatorial components near the cardiac frequency. We return to these questions and discuss them in more detail at the end of section 4.2. A quadratic interaction will give rise to higher harmonic components with frequencies $2f_1$, $2f_2$, $f_1 + f_2$ and $f_1 - f_2$, in addition to the characteristic frequencies (Fackrell 1996). As well as having a particular harmonic structure, the components also have phases that are related, $2\phi_1, 2\phi_2, \phi_1 + \phi_2$ and $\phi_1 - \phi_2$.

As discussed in detail by Jamšek *et al.* (2003), the bispectrum quantifies relationships among the underlying oscillatory components of the observed signals. Specifically, bispectral analysis examines the relationships between the oscillations at two basic frequencies, f_1 and f_2 and a modulation component at the frequency $f_1 \pm f_2$. This set of three frequencies is known as a triplet (f_1,f_2,$f_1 \pm f_2$).

A high bispectrum value at bifrequency (f_1, f_2) indicates that there is at least frequency coupling within the triplet of frequencies f_1, f_2, and $f_1 \pm f_2$. Strong coupling implies that the oscillatory components at f_1 and f_2 may have a common generator, or that the cardiovascular circuit they drive may, through a non-linear interaction, synthesize a new, dependent component at frequency, $f_1 \pm f_2$.

Nonlinear transformation causes the appearance of self-coupling peaks in the bispectrum (Nikias and Petropulu 1993, Zhou and Giannakis 1995). In periodic signals, peaks at the self-frequency without self-phase couplings are common. Again, the simultaneous appearance of both couplings is a very strong indicator of the presence of nonlinearity.

2.1. Measurements

The data acquisition techniques have already been described (Stefanovska and Bračič 1999) but, in summary, were as follows. A four-channel laser Doppler blood flow

monitor (floLAB, Moor Instruments Ltd., UK) was used for simultaneous recordings of blood flow at the four different sites: both arms (left and right caput ulnae) and both legs (left and right medial maleollus). Skin over bony prominences was chosen in order to standardize the measurement sites for the four extremities. A standard calibration (flux standard) of all the probes was made in order to be able to compare signals, and the blood flow was expressed in arbitrary units (AU). The electrical activity of the heart (ECG), respiration and blood pressure were also simultaneously recorded. The respiratory effort was measured using the TSD101B Respiratory Effort Transducer (Biopac Systems, Inc., USA). It consists of a piezoresistive sensor equipped with a silicon rubber strain assembly that measures the change in thoracic or abdominal circumference. The electrical conductivity of the sensor is proportional to the increase of abdominal circumference. The blood pressure was also measured with a piezoelectric transducer, and the ECG was recorded using a standard technique with two electrodes placed on the shoulders and one below the heart.

Six males aged 25–27 years with no history of cardiopulmonary disease participated in the study. Each of them lay in repose on a bed for 15 minutes before the start of data recording. One set of measurements was taken in the normal relaxed state, with spontaneous breathing, and a further two/three measurements under differently paced breathing. The duration of the measurements was 20 min for spontaneous breathing, and 12 min for paced breathing. Blood flow signals were digitized with 16-bit resolution and sampled at 40 Hz, whereas the ECG, respiration and pressure signals were sampled at 400 Hz. The paced respiration frequency was held constant during the measurement of a given time series and the rhythm was paced by metronome. Altogether 22 recordings were made, as summarized in Table 1.

2.2. Data analysis

The blood flow signals were first pre-processed. Both very low and very high frequencies were removed by use of moving average windows: drift with a 200 s long window; and high frequencies with a 0.2 s window while, and at the same time, the signal was resampled to 10 Hz. By using the moving average before resampling, we avoid problems of aliasing. In addition, each signal was normalized to lie between zero and one, and its mean value was then subtracted. The characteristic cardiac f_1 and respiratory f_2 frequencies, and their components at harmonically related positions, were identified: for each signal, the power spectrum was computed to identify f_1 and f_2, and to detect those components possibly caused by nonlinear interactions, $2f_1$, $2f_2$, and $f_1 \pm f_2$. Then the bispectrum was calculated. For each time series the signal was divided into several segments and to ensure stationarity the average value within each window was also subtracted. The chosen window length affected both frequency resolution and the statistical stability of the estimates. Because of the finite length of the time series, optimal choice of the number of segments requires a measure of compromise: the more segments the better the estimates, but increasing the number of segments also reduces the length of individual segments which, in turn, reduces the frequency resolution. To obtain reliable estimates 30 or more segments are necessary (Jamšek *et al.* 2003). The compromise can be optimised by an appropriate overlapping of the segments (see below).

In the case of quadratic coupling, for which we wish to test, several peaks occur in the bispectrum. Besides those at the bifrequencies (f_1, f_2), the cardiac self-coupling

Table 1.
Data for six subjects measured during spontaneous and paced respiration. $\overline{V_T}$ is average tidal volume, $\sigma_{\overline{V_T}}$ is its standard deviation, f_1 is average heart frequency and f_2 is average respiratory frequency during spontaneous f_{2_s} and paced f_{2_p} respiration. The tidal volume is obtained as a value between minimum voltage recorded during expiration and a succeeding maximum voltage recorded during inspiration. The voltages were not calibrated to express volumes in litres; rather, values were normalized to the average tidal volume obtained for each subject during spontaneous respiration. Data marked with $*$ are presented in Table 3.

Person	Breathing	Age (yr)	f_1 (Hz)	f_2 (Hz)	$\overline{V_T}/V_{T_s}$	$\sigma_{\overline{V_T}}/V_{T_s}$	Note
1	f_{2_s}	27	1.10	0.13	1.00	0.27	
	$f_{2_p} < f_{2_s}$		1.08	0.11	1.31	0.17	*
	$f_{2_p} > f_{2_s}$		1.00	0.23	1.08	0.18	*
	$f_{2_p} > f_{2_s}$		0.97	0.34	2.56	0.68	*
2	f_{2_s}	27	1.16	0.14	1.00	0.13	*
	$f_{2_p} < f_{2_s}$		1.06	0.09	1.33	0.22	
	$f_{2_p} < f_{2_s}$		1.05	0.10	0.83	0.11	*
	$f_{2_p} < f_{2_s}$		0.98	0.11	0.67	0.10	*
3	f_{2_s}	25	1.03	0.16	1.00	0.20	
	$f_{2_p} < f_{2_s}$		1.08	0.13	1.40	0.11	*
	$f_{2_p} > f_{2_s}$		1.10	0.26	0.95	0.23	*
4	f_{2_s}	25	0.99	0.16	1.00	0.20	
	$f_{2_p} < f_{2_s}$		1.01	0.10	1.82	0.28	*
	$f_{2_p} < f_{2_s}$		0.99	0.11	1.88	0.12	*
	$f_{2_p} > f_{2_s}$		1.03	0.20	1.08	0.26	
5	f_{2_s}	26	1.20	0.15	1.00	0.49	
	$f_{2_p} < f_{2_s}$		1.20	0.10	4.31	0.90	*
	$f_{2_p} < f_{2_s}$		1.20	0.11	1.84	0.70	
	$f_{2_p} > f_{2_s}$		1.14	0.21	0.44	0.12	
6	f_{2_s}	25	0.95	0.27	1.00	0.22	
	$f_{2_p} > f_{2_s}$		0.89	0.35	0.15	0.07	
	$f_{2_p} < f_{2_s}$		0.92	0.24	0.55	0.11	

Table 2. Peaks at bifrequencies in the bispectrum, arising as the result of a nonlinear interaction between the two oscillators f_1 and f_2.

Peak	Bifrequency
1	(f_1, f_2)
2	$(f_1 - f_2, f_2)$
3	$(f_1 - f_2, 2f_2)$
4	$(f_1, 2f_2)$
5	$(f_1, f_1 - f_2)$
6	$(f_1 + f_2, f_1 - f_2)$
7	(f_2, f_2)
8	(f_1, f_1)

(f_1, f_1) and respiration self-coupling (f_2, f_2), others occur because of the interactions. Those of primary interest were at bifrequency (f_1, f_2), representing the coupling between the two oscillators, and five others. To investigate the cardio-respiratory coupling 8 peaks were analyzed for each signal, as shown in Table 2. To be able to

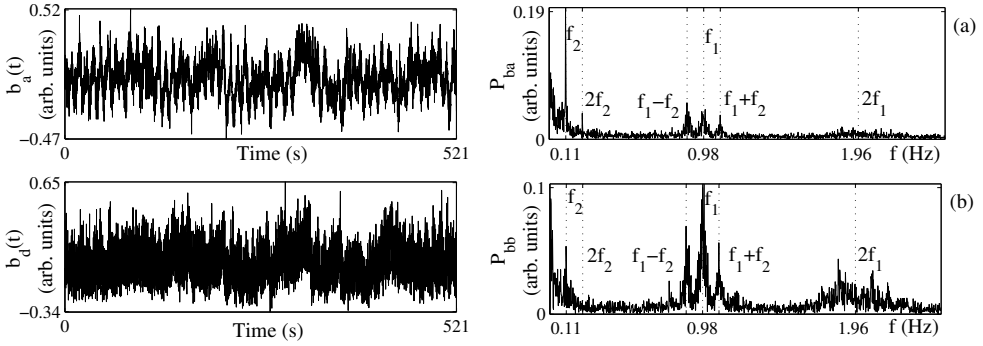

Figure 1. Blood flow signals $b(t)$ measured simultaneously, after preprocessing (left), and their power spectra (right): (a) from the right wrist $b_a(t)$ (channel a); and (b) from the left ankle $b_d(t)$ (channel d).

compare results, a normalization procedure was performed (see Appendix A).

The maximum biphase and biamplitude were calculated for each peak. The frequency resolution was set at 1/10 of the lowest respiration frequency or better. The slowest-paced breathing, f_2, was around 0.1 Hz, so that a window of 100 s or longer was necessary for estimation of the bispectrum, biphase and biamplitude. Short plateaus in the estimated biphase occur frequently. To exclude coincidence interactions we focused on those that lasted for at least 10 periods of the lower coupling frequency f_2. The length of the window also determines the time resolution. In the case of the slowest-paced breathing, we were seeking $\sim 10 \times (1/f_2) = 100\,\mathrm{s}$ long epochs of constant biphase. Therefore a window length of 100 s or less was necessary to meet the criterion for time resolution. Due to the Heisenberg uncertainty principle (Kaiser 1994), the scope for choice of window length is limited, and compromise is needed between time and frequency resolution. The window was moved along the time series with a minimum time step of $1/f_s = 0.1\,\mathrm{s}$, where f_s is the sampling frequency. The critical value for the biamplitude estimate to be considered valid was set in all cases to 2, i.e. twice the average value of the bispectrum within its so-called inner triangle (IT), as discussed in Appendix A.

To be able to conclude that quadratic coupling exists, we require several condition to be fulfilled: (i) a constant biphase during at least 10 periods of the lower-frequency interacting component; (ii) biphases for all six (8) peaks must be present at the same time as the biphase plateau; (iii) no phase slips must occur during the coupling, and the biphase variations must stay within a π rad interval (the biphase being expected to be more or less constant, depending on the coupling strength and noise intensity: phase slips are frequent when the interaction is extremely weak; they are mostly due to noise, but sometimes caused by modulation; strong modulation is expected to result in a biphase with fewer phase slips); (iv) The biamplitude must be above the chosen critical value, i.e. be more than twice the average bispectrum value within the IT.

3. Results

Examples of blood flow signals after preprocessing are presented in the left-hand column of Fig. 1. These signals correspond to the case of paced respiration slower

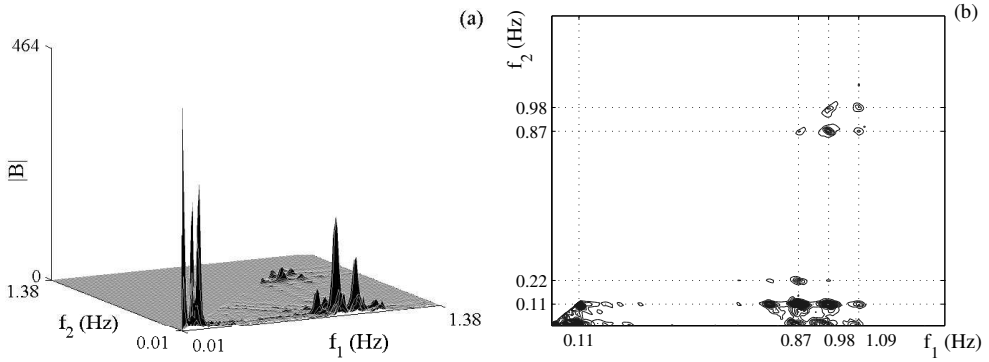

Figure 2. (a) Part of the bispectrum $|B|$ for a signal b_a, calculated with $K = 33$ segments, 87 % overlapping and using the Blackman window to reduce leakage. (b) its contour view.

than the natural frequency. Their calculated frequency content is presented in the right hand column. The peak at ∼0.98 Hz belongs to cardiac activity, f_1; that at ∼0.11 Hz to respiratory activity, f_2, which was also obtained directly as a check by use of a piezo sensor. Although the characteristic frequencies differ from person to person, they all lie within defined frequency bounds. Stefanovska and Bračič (1999) proposed that the respiration frequency interval should be defined as 0.14–0.6 Hz with a median frequency 0.3 Hz. The spontaneous respiratory frequency for person 2 was 0.14 Hz, i.e. it fell at the lower limit of this interval. The slowest *paced* respiration frequency was set to 0.09 Hz.

Assuming nonlinear cardio-respiratory coupling the cardiac side peaks are positioned at their sum $f_1 + f_2 \simeq 1.09$ Hz, and difference $f_1 - f_2 \simeq 0.87$ Hz. Cardiac $2f_1$ and respiratory $2f_2$ second harmonics are also present. It can be seen that their precise values vary in time, which is what makes the analysis difficult. The widths of the peaks indicate their time-variable frequency content, which makes a time-frequency domain presentation more convenient (Kaiser 1994, Bračič *et al.* 2000). The effect is, of course, associated with the interactions between the cardiovascular oscillators.

A typical bispectrum for the whole frequency domain for signal b_a is presented in Fig. 2. A very high peak located at bifrequency (0.11 Hz, 0.11 Hz), belonging to the respiratory self-coupling can be seen. At least four other peaks are clearly evident: at (0.98 Hz, 0.11 Hz) attributable to cardio-respiratory coupling; at (0.87 Hz, 0.11 Hz) which we assume to be coupling between the respiratory component f_2 and the difference $f_1 - f_2$, that could be due to a nonlinear coupling mechanism; and two peaks attributable to interaction with lower cardiovascular characteristic components. The latter interactions (with the intrinsic myogenic and neurogenic oscillators) are not of interest in the present context. Also, other lower frequency peaks can be seen in the bispectrum. Their positions can be seen in the bispectrum contour view shown in Fig. 2(b).

The bispectrum is sensitive to time-variations of the frequency components, yielding in the bispectrum a characteristic diagonal elongation of peaks. The cardiac frequency f_1 spans 0.93–1.02 Hz. Although the respiratory frequency f_2 extends from 0.09 Hz to 0.12 Hz, this large range is actually the result of a single deep breath:

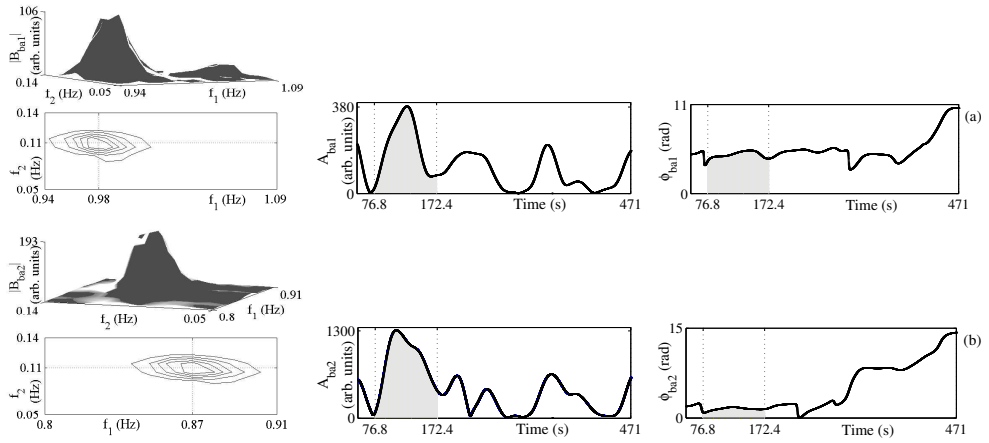

Figure 3. Examples of blood flow analyses for signal $b_{a(t)}$, calculated with $K = 33$ segments, 87 % overlapping, using a 0.1 s time step and a 100 s long window for estimating the DFT, with a Blackman window to reduce leakage, for peaks (a) 1 and (b) 2. The left column shows the bispectrum $|B_{b_a}|$ with its corresponding contour plots; middle, the biamplitude A_{b_a}; and right, the biphase ϕ_{b_a}.

the respiratory frequency (being paced) is constant for most of the time, leading to a high bispectrum. The cardio-respiratory bifrequency coupling consequently has a wide frequency range resulting mainly from variation of the cardiac frequency (in Fig. 2 it is elongated along the f_1 axes). The peaks corresponding to cardiac activity are lower, mainly due to time frequency variations. In the presence of quadratic nonlinear coupling, peaks should be present at all six of the bifrequencies summarized in Table 2. Significant values of the bispectrum (i.e. exceeding twice the average bispectrum within the IT) were obtained near all these bifrequencies (see the left-hand column of Fig.3, showing that the peaks are indeed present.

Once the peaks at the defined bifrequencies had been confirmed, the time biphase and biamplitude were calculated at the bifrequency peaks. It can be seen that the biamplitude during the time interval from 76.8 s to 172.4 s meets our criterion of being more than twice as large as the average bispectrum in the IT: see middle column of Fig. 3. The biphase in this time interval, 95.6 s long (shaded area), remains constant within a 1.47 rad interval, i.e. there are no phase slips. The biphases at bifrequencies 1, 2, 3 and 5 are very constant; those at 4 and 6 are less so, but they still remain within the π rad interval.

3.1. Global couplings

Blood flow signals reflect local characteristics, but those derived from widely separated sites can be remarkably similar. Although they reflect the flow in the capillary bed, each of them contains the same information on the spatially invariant periodic activities seen in the centrally generated cardiac and respiratory signals. The power of each oscillatory component in the peripheral blood flow varies with the vessels' diameters and the network density, i.e. the local resistance to the flow. The choice of measurement sites to have similar network density was based on human anatomy, viz.

on both wrist and ankle joints (Stefanovska and Bračič 1999, Bračič *et al.* 2000).

Our measured signals, i.e. channels a to d, come from widely differing sites. Nonetheless, in agreement with the earlier work, the respiratory and cardiac characteristic frequency components preserve the same values and, moreover, their phase relationships contain the same information. The left-hand column of Fig. 4 shows the bispectrum for peak 1 for signal b_d measured on channel d. The maximum amplitude of the peak is positioned at the same bifrequency (0.98 Hz, 0.11 Hz) as already seen for peak 1 of signal the b_a measured on channel a. The correlation of the biamplitude and biphase for signals b_a and b_d is very high, both being 0.85, as can also be seen from their time evolution presented in the right-hand and middle column of Fig. 4. The biamplitude meets our amplitude criterion within the same time interval from 76.8 s to 172.4 s during which the biphase is also constant. We obtain the same coupling information at all 4 measuring sites for all the peaks (1-8). The results obtained from time-bispectral analyses of the measured signals are summarized in Table 3. Inspecting the data in Tables 1 and 3 we see no obvious correlation between the average tidal volume and the occurrence of nonlinear cardio-respiratory interaction.

3.2. Cross-bispectrum

The bispectrum as defined in (Jamšek *et al.* 2003) can be seen as a special case of the cross-bispectrum when the three signals are the same. In addition to the blood flow signals, the ECG $e(t)$, respiration $r(t)$ and blood pressure $p(t)$ were also simultaneously recorded. This gave us the possibility of globally checking the coupling between cardiac and respiratory activity, using bivariate data. Let us define the cross-bispectrum as

$$B_{xyy}(k,l) = X(k)Y(l)Y^*(k+l) \tag{1}$$

where X and Y are discrete Fourier transforms (DFTs) of two different signals $x(t)$ and $y(t)$ at discrete frequencies k, l and $k+l$. We calculated the cross-bispectrum B_{cebb} (where c stands for cross, e for signal $e(t)$ and b for signal $b(t)$), for the case where $x(t)$ is the ECG signal $e(t)$ and $y(t)$ is the blood flow signal $b_a(t)$. The ECG signal tells us primarily about the cardiac electrical activity. The phase of the first, cardiac component f_1, in the triplet (f_1, f_2, f_1+f_2) is thus directly extracted from the ECG signal. The respiratory component f_2 and the component at the harmonically related position $f_1 + f_2$ are extracted from the blood flow signal.

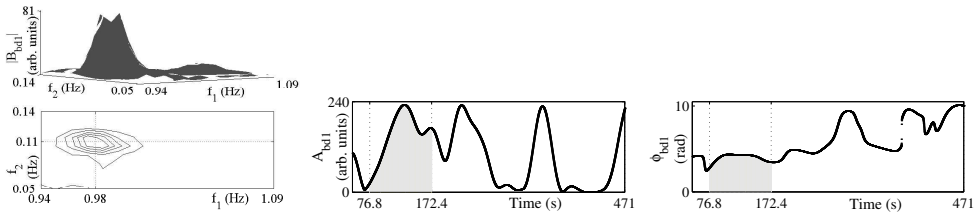

Figure 4. Left: the bispectrum $|B|$ calculated with $K = 33$ segments, 87 % overlapping and using the Blackman window to reduce leakage for the signal b_d for peak 1 with its contour view. Middle: the biamplitude A, and right the biphase ϕ; a 0.1 s time step and 100 s long window were used for computation of the DFT using a Blackman window.

Table 3. Quadratic nonlinear couplings detected in blood flow signals marked by $*$ in Table 1. For each measurement, four blood flow signals were measured simultaneously at different sites, channels a-d. T_{qc} is the time interval during which the bispectral analysis showed that the heart oscillator f_1 and the respiratory oscillator f_2 might be nonlinear coupled. The product of $T_{qc} \times f_2$ tells us over how many respiratory periods the interaction persisted. During T_{qc} the maximum biamplitude is calculated for the peak 1 that is of our primary interest. In addition, the maximum variation of the biphase $\Delta\phi$, its average value $\overline{\phi}$, and its standard deviation σ_ϕ were calculated during T_{qc}.

Person	Breathing	Chan.	f_1 (Hz)	f_2 (Hz)	T_{qc} (s)	$T_{qc} \times f_2$	$A1_{max}$ (A.U.)	$\Delta\phi$ (rad)	$\overline{\phi}$ (rad)	σ_ϕ (rad)
1	paced	a	1.08	0.11	105.7	11.6	190	1.11	8.92	0.20
	paced	d	1.00	0.23	56.8	13.1	62	0.92	10.93	0.29
	paced	b	0.97	0.34	18.9	6.4	50	0.84	0.47	0.28
2	spont.	a	1.16	0.14	82.0	11.5	352	1.87	32.68	0.47
	paced	c	1.05	0.10	89.5	9.0	122	1.48	4.05	0.34
	paced	a	0.98	0.11	95.6	10.5	383	1.47	3.22	0.42
3	paced	d	1.08	0.13	56.5	7.3	334	1.29	2.21	0.48
	paced	c	1.10	0.26	52.4	13.6	52	0.46	4.96	0.10
4	paced	d	1.01	0.10	105.6	10.6	407	2.47	0.58	0.18
	paced	d	0.99	0.11	95.6	10.5	219	2.19	-6.51	0.76
5	paced	d	1.20	0.10	57.5	5.8	1009	2.05	5.88	0.67

We also define the cross-bispectrum

$$B_{xyx}(k,l) = X(k)Y(l)X^*(k+l) \tag{2}$$

and calculate it for 2 different cases: (i) B_{cbrb}, where $x(t)$ is the blood flow signal $b_a(t)$ and $y(t)$ is the respiration signal $r(t)$. The signal $r(t)$ describes most directly the activity of the respiratory oscillator. Therefore the phase of the second component in the triplet (f_1, f_2, $f_1 + f_2$) is directly extracted from the respiratory signal. (ii) B_{cprp}, where $x(t)$ is the blood pressure signal $p(t)$ and $y(t)$ is the respiration signal $r(t)$. By calculating the latter cross-bispectrum we are interested in establishing whether the information about coupling between the heart and the respiratory oscillators is signal-independent.

We proceeded as discussed above in section 2.2 for each of the three different cross-bispectrum cases. The time evolution of the signals $e(t)$, $r(t)$ and $p(t)$ and their power spectra are presented in Fig. 5 (a) and (b). For the cross-bispectrum B_{cebb} all the peaks from 1 to 8 are present at the same bifrequencies as in the case of auto-bispectrum of the blood flow signal. Since the power spectrum of the respiratory signal P_r exhibits only components of the respiratory oscillator we cannot expect peaks 5, 6 and 8 to appear in the cross-bispectra B_{cbrb} and B_{cprp}. All the other peaks are present at the same bifrequencies as in the auto-bispectrum. The biamplitude meets our amplitude criterion within the same time interval from 76.8 s to 172.4 s, for all peaks; moreover the biphase is constant during this time interval. Examples of the biamplitude and biphase time evolution for peak 1 for the three different cross-bispectra are presented in Fig. 5 (c) and (d).

Cross-bispectra were also calculated with surrogate data, where the phases of the frequency components of the signals $e(t), r(t)$ and $p(t)$ were randomized. No phase couplings were detected in this case. The coupling information among cardiac and respiratory process seems to be signal independent.

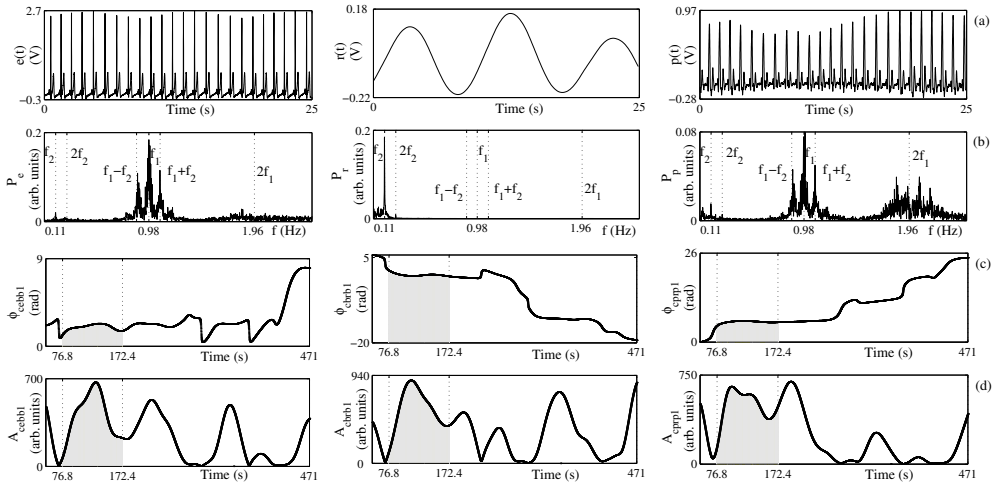

Figure 5. Results for the cross-bispectrum. Row (a) shows the first 25 s of the signals: left ECG signal $e(t)$, middle respiration signal $r(t)$, and right differentiated blood pressure signal $p(t)$; whereas row (b) shows their power spectra. The sampling frequency was $f_s = 400\,Hz$. In the lower rows (c) the biphase ϕ and (d) the biamplitude A are shown; a 0.1 s time step and 100 s long window were used for computation of the DFT using a Blackman window. The biphase and the biamplitude were calculated using the cross-bispectra (left) B_{ebb}, (middle) B_{brb} and (right) B_{prp}.

4. Discussion

The signals were measured from six persons, whereas in the first column of table 3 data are only provided for five; the sixth person also showed evidence of nonlinear couplings, but over time intervals that were too short to fulfil our required conditions. Four blood flow signals simultaneously measured in different places (channels a, b, c, and d) were available for each recording. We usually analyzed first the one with the most distinctive characteristic frequencies in its power spectrum and, if our criteria were fulfilled, we checked the other three signals as well. The time interval T_{qc} during which quadratic coupling persisted was determined; if all 6 peaks fulfilled our conditions, then the T_{qc} interval was calculated for all peaks and the boundaries were defined such that the biamplitude for all the peaks in T_{qc} interval would be above the condition.

Also shown in Table 3 are three cases where the couplings T_{qc} lasted less than $10 \times 1/f_2$, where $1/f_2$ is the longest respiratory period, since they could be detected very distinctly and clearly. Column $A_{1_{max}}$ is the maximum biamplitude for peak 1 during the T_{qc} interval. The strength of the coupling is in general not correlated with its duration. For each T_{qc} interval, the maximum variation $\Delta\phi$ of the biphase, its average value, and its standard deviation, were calculated. There was a single case (only) of spontaneous breathing for which the coupling lasted long enough (82 s without phase slips) to fulfil our criteria; during spontaneous respiration phase slips are relatively frequent and epochs of constant biphase are short.

4.1. Definition of the phase

As mentioned above in section 1, the cardiac and respiratory systems can be perceived as coupled autonomous oscillators. Using a bispectrum based on the Fourier transform, which is a decomposition of the signal in terms of complex exponential (sinusoidal) components, each component can be represented as a point in a complex space, $\Re[X(k)]$ versus $\Im[X(k)]$, thus defining a vector, where X is DFT and k is a discrete frequency. Its magnitude represents a power, whereas the phase is determined by the angle between the vector and the positive real axis. The phase of an oscillator is defined as the phase of the sinusoidal component that lies closest to its characteristic frequency. Thus our phase definition differs from that used in Kuramoto phase reduction (Kuramoto 1984). In this way it is possible to study the phase relations and to resolve the nature of the couplings.

4.2. Nonlinear coupling, or linear coupling of strongly nonlinear oscillators?

Our study is based on the assumptions that the cardiac and respiration processes can be described as weakly nonlinear oscillators and that the interaction between them is also weak (Stefanovska *et al.* 2001b). It is pertinent to investigate what happens when these assumptions are *not* fulfilled. We have addressed the question in two different ways based on analytic approximation and digital simulation, respectively.

The analysis in Appendix B considers harmonic generation by a pair of coupled, weakly nonlinear, oscillators. It confirms that, for weak coupling, the appearance of additional harmonics at $2w_2$, $2w_1$, $2w_1 \pm 2w_2$, $w_1 \pm w_2$, $3w_1 \pm w_2$ can confidently be associated with the presence of quadratic coupling. For a sufficiently nonlinear oscillator and sufficiently strong coupling, these and other combinatorial harmonics can in principle be generated, as a second order effect, even for linear coupling. As will be illustrated below, however, the appearance of these combinatorial harmonics does not in itself fulfil the necessary conditions to support a conclusion that there is nonlinear coupling when tested by bispectral analysis: the high biamplitude and constant biphase may be absent. In any case, the bispectral approach cannot be expected to yield reliable information about the nature of the coupling when the nonlinearities are extremely strong.

We have therefore complemented the analysis of Appendix B with a digital simulation, exploring the range of extreme conditions where the bispectral approach is expected to fail. We have chosen to simulate a generic model (3) of the van der Pol relaxation oscillator, with an additional nonlinear term, linearly driven by another relaxation van der Pol oscillator via an additive coupling

$$\begin{aligned} \dot{x_1} &= y_1 \\ \dot{y_1} &= \varepsilon_1(1-x_1)^2 y_1 - \omega_1^2 x_1 + \eta_1 x_1^2 + \mu_1(x_1 - x_2) + \xi(t) \\ \dot{x_2} &= y_2 \\ \dot{y_2} &= \varepsilon_2(1-x_2)^2 y_2 - \omega_2^2 x_2. \end{aligned} \tag{3}$$

The activity of the oscillators is described by the two state variables x_i and y_i, and ε_i and $\omega_i = 2\pi f_i$ are constants, where $i = 1, 2$ denote respectively the driven or the driving oscillator. η_1 is a constant that sets the strength of the additional nonlinear term in the driven oscillator, and μ_1 is the strength of the coupling. Here $\xi(t)$ is zero-mean white Gaussian noise, $\langle \xi(t) \rangle = 0$, $\langle \xi(t), \xi(0) \rangle = D\delta(t)$ and $D = 0.8$ is the noise

intensity. Following the pioneering work of van der Pol and van der Mark (1928), the parameters are set to $\varepsilon_1 = 70$, and $\varepsilon_2 = 3$.

A detailed parameter space analysis has been completed, showing that a situation indeed exists for which the bispectral technique fails to distinguish between the two situations when: (i) two oscillators are *strongly* nonlinear, but linearly coupled; or (ii) when they are nonlinear and nonlinearly coupled. As an illustration, bispectral analysis was performed for two coupled van der Pol oscillators, with and without added Gaussian noise, for different sets of parameters. In the first case the strength of the additional nonlinearity was changed, while μ_1 was kept constant: (a) $\mu_1 = \text{const} = 1$; η_1 was 0, 0.5, 1, 2, 5, 10, 12 and 15, and from 20 to 90 was varied with step 10 and 93 was also included. (b) $\mu_1 = \text{const} = 25$; η_1 was varied from 1 to 10 with step 1, values 12, 15, 18 and 25 were also considered, and again values from 20 to 60 with step 10. In the second case the strength of the coupling was changed while η_1 was kept constant: (a) $\eta_1 = \text{const} = 1$; μ_1 was varied from 0.1 to 1 with step 0.1, from 1 to 10 with step 1, then values 2.5, 3.5, 11, 15, 20, 25, 30, 35, 120 and 200 were considered, and again values from 40 to 100 with step 10. (b) $\eta_1 = \text{const} = 5$; $\mu_1 = 25$. (c) $\eta_1 = \text{const} = 15$: μ_1 was varied from 1 to 10 with step 1, values 12, 15, 17, 20, 24 and 25 were considered, and again from 30 to 60 with step 10.

The test signal $x_a(t)$ is the variable x_1 of the driven oscillator, recorded as a continuous time series. For the first 400 s, the strength of the additional nonlinear term, i.e. $\eta_1 = 15$ was very strong and the coupling, i.e. $\mu_1 = 1$ was relatively strong; μ_1 was then substantially increased to 25, whereas the strength of the additional nonlinear term was decreased to 1. After a further 400 s, the strength of the additional nonlinear term was increased back to 15. The first 5 s and corresponding power spectrum for each coupling strength are shown in Fig. 6(a) and (b). The peak 1.1 Hz in the absence of coupling, labelled as f_1, represents the driven cardiac oscillator; and $f_2 = 0.24$ Hz represents the driving respiratory oscillator. These frequencies are deliberately chosen such that their ratio is not an integer.

The power spectra for all the three different cases of the strengths of the linear coupling and additional nonlinear term exhibit rich frequency content. As the coupling gets stronger, and/or the strength of the additional nonlinear term increases, the frequency content of the signal x_a becomes richer. The power spectra clearly exhibit components at the harmonically related positions $f_1 + f_2$ and $f_1 - f_2$.

The principal domain of the bispectrum for the test signal x_a, Fig. 6 (c) and (d), shows a peak at the bifrequency (0.96 Hz, 0.24 Hz) that is of our primary interest. A window length of 100 s was chosen to calculate the instantaneous biphase and biamplitude, Fig. 6 (e) and (f), and was moved across the signal in 0.1 s steps. The whole signal is analyzed as a single entity, but transients caused by the changes in coupling and/or in the strength of the additional nonlinear term are removed prior to processing.

During the period of relatively weak coupling $\mu_1 = 1$ and strong nonlinearities, no peak is present in the bispectrum as can be seen from the biamplitude, Fig. 6 (f), which remains far below unity (0.012). Moreover, at value $\eta_1 = 0.7$ the frequency component at modulation position $f_1 + f_2$ appears in the power spectrum for the first time. The modulation components $f_1 \pm f_2$ become large and almost equal in size in the power spectrum, but not until $\eta_1 = 15$. However, even then, not all the necessary peaks (also peak at bifrequency $(f_1, 2f_2)$) in the bispectrum are present and the method correctly resolves the absence of nonlinear coupling, even though the biphase is constant, Fig. 6 (e).

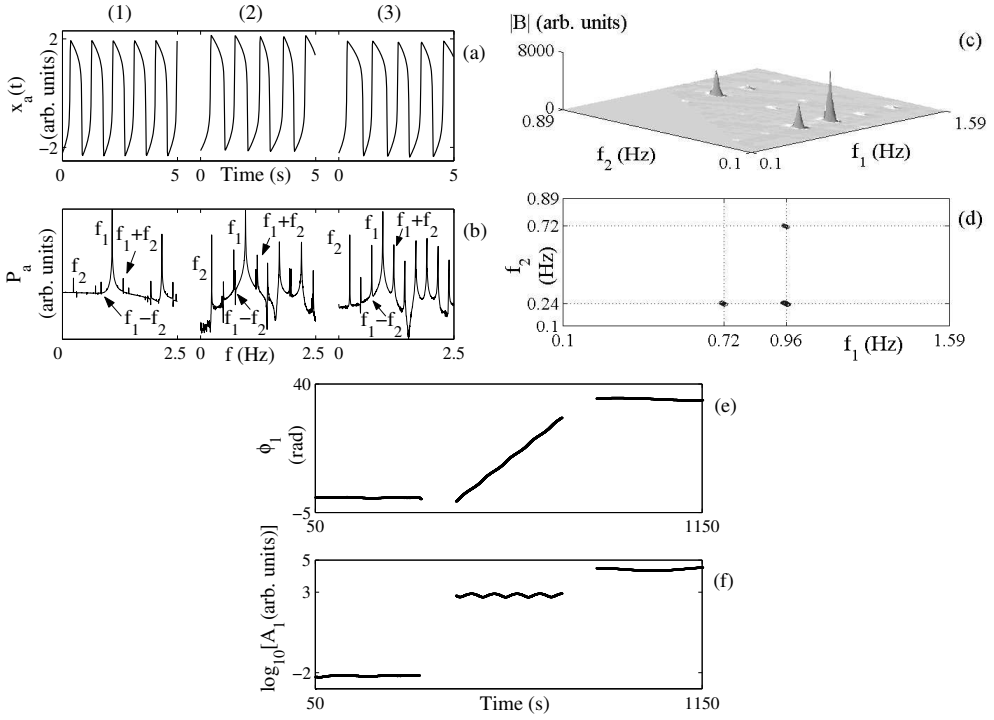

Figure 6. Digital simulation illustrating a situation where the bispectral method fails. The simulation models two unidirectionally, *very* strongly coupled, relaxation van der Pol oscillators with additional *very* strong nonlinear terms, in the presence of additive Gaussian noise. (a) The test signal x_a, of variable x_1 of the forced van der Pol oscillator with characteristic frequency $f_1 = 1.1\,\mathrm{Hz}$ periodicaly forced at frequency $f_2 = 0.24\,\mathrm{Hz}$ for three different coupling strengths $\mu_1 = 25$ (1), 1 (2), and 25 (3), with strengths of the additional nonlinear term $\eta_1 = 1$ (1), 15 (2), and 15 (3). Each coupling lasts for 400 s, at sampling frequency $f_s = 50\,\mathrm{Hz}$. Only the first 5 s are shown in each case. (b) The power spectrum of x_a . (c) Its bispectrum $|B|$ calculated with $K = 34$ segments, 67 % overlapping and using the Blackman window to reduce leakage and (d) its contour view. (e) The biphase ϕ and (f) the biamplitude A for bifrequency (0.96 Hz, 0.24 Hz), with a 0.1 s time step and a 100 s long window for estimating the DFTs using the Blackman window, for cases (1), (2) and (3). Note that only for (3) are both conditions (i.e. high enough biamplitude, and constant biphase) for the (incorrect) inference of nonlinear coupling satisfied.

By grossly exaggerating the strength of the coupling, with $\mu_1 = 25$, the frequency components that might also arise from nonlinear coupling become large. This results in substantial increases of the biamplitude at bifrequency (f_1, f_2) in the bispectrum; the biphase is then non-constant, however, and increases continuously. Again the required conditions for the identification of nonlinear coupling are not fulfilled.

In the most extreme example shown, with very strong coupling and very strong additional nonlinearity, i.e. with $\eta_1 = 25$, $\mu_1 = 25$, we are unable to distinguish between strong nonlinearity of the oscillators and strong nonlinear coupling. In a signal coming from a "black box", the observed frequency components could mistakenly be attributed to nonlinear coupling: the bispectrum, Fig. 6 (c), contains all the necessary

peaks (only three of them are visible, the rest of them being much smaller, although fulfilling the necessary amplitude condition). There are other frequency components that could result from nonlinear coupling, and the biphase remains constant. In this case the method clearly fails.

There are, however, compelling arguments suggesting that the cardiac and respiratory subsystems should be in fact treated as weakly nonlinear oscillators that are weakly coupled. (i) in healthy subjects, breathing spontaneously, only *occasional* and *brief* episodes of synchronization are seen (Schäfer *et al.* 1998, 1999, Bračič Lotrič and Stefanovska 2000), indicative of relatively weak coupling. (ii) Sinus arrhythmia is small at spontaneous breathing frequencies and only slightly larger at very low breathing frequencies (Eckberg 2003), again supporting a weak-coupling description. (iii) The couplings can sometimes decrease almost to vanishing point, e.g. in coma (Stefanovska and Bračič 1999). Without couplings, the dynamics becomes drastically simplified – with complete absence of synchronization or modulation. The fact that virtually no variability is seen in any of the natural frequencies, despite small amplitude variations attributable to internal noise, suggests that the oscillators themselves are at most weakly nonlinear. (iv) If there were strong oscillator nonlinearity, and strong (but linear) coupling, we would observe many combinatorial components around the cardiac frequency, which is not the case (see Fig. 1(a)-(d)). The excessively strong-coupling regime explored in the above simulations would appear, therefore, to be largely irrelevant to the cardio-respiratory interaction that we study in this paper: our bispectral technique (Jamšek *et al.* 2003) should be applicable as we have assumed.

4.3. Unidirectional or bidirectional coupling

We have studied the combinatorial frequencies that arise from the influence of the respiratory on the cardiac system. This naturally begs the question of whether the coupling is unidirectional or bidirectional. Using the same method one could equally well analyse the combinatorial frequencies responsible for the influence of cardiac on the respiratory system. In fact, using newly developed algorithms for analysis of the direction of coupling (Schreiber 2000, Rosenblum and Pikovsky 2001, Rosenblum *et al.* 2002, Paluš *et al.* 2001), it has already been shown (Stefanovska 2002, Paluš and Stefanovska 2003) that the two systems are *bidirectionally* coupled. The effect of respiratory system is, however, dominant (i.e. is the driving system) at all respiratory frequencies, whether paced or spontaneous.

Although during paced respiration the respiration frequency is kept constant, the situation differs markedly from that of a forced oscillator (with the cardiac oscillator being driven, and the respiration oscillator being the driver). Paced respiration experiments can in fact be perceived as a state of the system of two coupled oscillators where, although the frequency of one of them (respiration) is forced and kept constant, the interaction between the two oscillators remains spontaneous.

5. Summary and conclusions

The blood flow signal contains a great deal of information and is exceptionally challenging in relation to processing. It possesses components whose amplitudes and frequencies vary in time. Moreover, the interactions among its characteristic oscillations also vary in time, and their nature (frequency, phase, linear and/or

quadratic couplings) also changes giving rise to the observed complexity of cardiovascular dynamics.

Bispectral analysis has provided insight into the nature of the couplings. Our results support the inference that the dynamics of blood flow can usefully be considered in terms of coupled oscillators. Application to the cardio-respiratory interaction has shown for the first time that nonlinear coupling is present. We have not sought evidence for couplings beyond second order, but higher order coupling may also exist.

We have shown that the effect of the coupling between the cardiac and respiratory oscillations is episodic, rather than fixed and permanent. Moreover, an interchange between frequency and phase couplings is also present, as demonstrated by the evolution of their time-biphase.

Nonlinear coupling was revealed, and shown to exist during spontaneous as well as during paced respiration. Episodes with nonlinear coupling were detected in 11 out of the 22 recordings and lasted between 19 s in case of high respiratory frequency ($f_{2_p} = 0.34$ Hz) to 106 s in case of low paced frequency of respiration ($f_{2_P} = 0.11$ Hz). The episodic nature of the cardio-respiratory interaction in a healthy human during spontaneous and paced respiration had already been demonstrated using quite different techniques of analysis (Kenner *et al.* 1976, Raschke 1987, Seidel and Herzel 1998, Schäfer *et al.* 1999, Bračič Lotrič and Stefanovska 2000, Rzeczinski *et al.* 2002). It allows us to infer that the inter-oscillator coupling is probably relatively weak.

Using bispectral and cross-bispectral analysis we have also shown that the coupling information among cardiac and respiratory processes is temporally and spatially invariant. Both processes are of central origin and their phase relationships can be observed in ECG, blood flow and blood pressure signals derived from widely separated sites. It would appear that the information is incorporated within the wave motion of the blood propagating through the vessels.

It is of interest to compare our experiment with that of Davies *et al.* (2000). They too studied physiological time series while respiration was being paced at a constant rate; in addition, they also guided the ventilatory amplitude (tidal volume) so as to produce a sinsusoidal modulation envelope of period 60 s. It resulted in oscillations of the same period in several physiological quantities, including the R–R intervals, blood pressure, and the cardiac stroke volume and output. In the present study, the ventilatory amplitude was left to the subject's spontaneous choice. The slow amplitude modulation of Davies *et al.* (2000) was selected to mimic the pattern of Cheyne-Stokes respiration often associated with heart failure. In our study, without any amplitude modulation, we were examining the question whether the relationship between cardiac and respiratory oscillations can be nonlinear. It is difficult to decide whether the nonlinear interactions, shown to occur episodically in the present study, would or would not have occurred if the amplitude of respiratory oscillations had also been controlled, as in the study by Davies *et al.* (2000). We have shown, however, that quadratic coupling exists even when both the frequency and the amplitude of respiration are spontaneous. We may therefore conclude that the nonlinear nature of the interaction between the cardiac and respiratory oscillations is inherent, and that it becomes more pronounced when the frequency of respiration is kept constant.

The questions of what the nonlinear couplings mean, and how they arise, are yet to be resolved. A full understanding of these couplings is essential to gain insight into the physiology and pathophysiology of cardiovascular dynamics, as well as for the construction of mathematical models offering novel possibilities for obtaining clinically

relevant physiological information. We conclude that bispectral analysis provides a promising tool for the determination of frequency and phase couplings in the processing and understanding of cardiovascular signals.

Acknowledgements

We gratefully acknowledge valuable discussions and correspondence with Yoshiki Kuramoto, Bojan Musizza and Yuri Shiogai. We are especially indebted to Andriy Bandrivskyy for his assistance in analysing harmonic generation by coupled oscillators. The study was supported in part by the Slovenian Ministry of Education, Science and Sport, by the Engineering and Physical Sciences Research Council (UK), by the British Council, by the Leverhulme Trust and by INTAS.

APPENDIX A: NORMALIZATION

Just as the discrete power spectrum has a point of symmetry at the folding frequency $f_s/2$, the discrete bispectrum has many symmetries in the k, l plane (Pflug *et al.* 1993, 1994). For real signals, the bispectrum has 12 symmetry regions. Because of these, it is necessary to calculate the bispectrum only in the non-redundant region, or principal domain. The latter can be divided into two triangular regions in which the discrete bispectrum has different properties: the inner triangle (IT), and the outer one (Hinich 1990, Sharfer and Messer 1993, Hinich and Messer 1995). In the current work it is the IT that is of primary interest. Thus it is sufficient to calculate the bispectrum over the IT of the principal domain defined in (Nikias and Petropulu 1993): $0 \leq l \leq k$, $k + l \leq f_s/2$.

To be able to compare results a normalization procedure was performed. For each bispectrum and biphase estimate, a bispectrum was first calculated for the whole IT using the same parameters, i.e. number of segments, segment length, percentage of segment overlap, type of tapering window, and size of window for frequency averaging. The normalization value was calculated as the average bispectrum estimate over the IT (Jamšek *et al.* 2003).

Normalization is parameter dependent. The more segments (short windows) for the bispectrum calculation, the higher its average value over the IT becomes. It has local maxima, because the width of the window directly affects the frequency resolution. The better the frequency resolution, the smaller the leakage effect. Higher percentages of overlap result in a lower average value over the IT, whereas the frequency averaging window increases the average value.

The normalized bispectrum also indicates the average level of quadratic nonlinear phase coupling and, in a way, serves as an indicator of how non-Gaussian the signal is (Hinich 1982).

The critical values for the bispectrum and biamplitude estimates were normalized to 1. If the estimated value is higher than the average value of bispectrum in the IT, then it is taken as valid. By critical value is meant a value that exceeds the leakage affect, the noisy background (other than Gaussian), and rounding errors.

APPENDIX B: GENERATION OF HARMONICS

In this appendix we show which harmonics appear in the spectrum of a weakly driven weakly nonlinear oscillator, and in particular we establish which harmonics correspond

to quadratic coupling. The analysis that follows is for a Poincaré oscillator, but a similar result also follows for e.g. a van der Pol or other oscillators of similar type.

Consider an oscillator of the form

$$\dot{x}_1 = -x_1 r_1 - w_1 y_1 + Q(x_2, x_1), \tag{4}$$

$$\dot{y}_1 = -y_1 r_1 + w_1 x_1, \tag{5}$$

$$r_1 = \alpha(\sqrt{x_1^2 + y_1^2} - a), \tag{6}$$

where the term $Q(x_2, x_1)$ corresponds to a coupling of the main oscillator (x_1, y_1) to another one (x_2, y_2).

We seek a solution in the form

$$x_1 = A\sin(w_1 t + \phi), \tag{7}$$

$$y_1 = -A\cos(w_1 t + \phi), \tag{8}$$

and transform equations (4)-(5) into amplitude/phase coordinates

$$\dot{A} = -\alpha A(A - a) + Q(x_2, A, \phi)\sin(w_1 t + \phi), \tag{9}$$

$$A\dot{\phi} = Q(x_2, A, \phi)\cos(w_1 t + \phi). \tag{10}$$

If there is no coupling ($Q(x_2, A, \phi) = 0$) this system has the simple solution

$$A = A_0 = a, \quad \phi = \phi_0 = const. \tag{11}$$

If the coupling is non-zero, the system cannot be solved exactly analytically. An approximate solution for small coupling and weak nonlinearity can, however, still be obtained. The amplitude and phase in this case vary only slightly and they can be expanded about $(A_0,\ \phi_0)$ as

$$A = A_0 + \beta, \quad \phi = \phi_0 + \gamma. \tag{12}$$

For small $\beta,\ \gamma,\ \alpha$ the equations (9)-(10) corresponding to those for $\dot{\beta}$ and $\dot{\gamma}$ can be solved approximately. For the simplest linear coupling of form

$$Q(x_2, A, \phi) = Q(x_2) = F\sin(w_2 t) \tag{13}$$

one obtains

$$\beta \approx \frac{F}{2(w_1 - w_2)}\sin((w_1 - w_2)t + \phi_0)$$
$$-\frac{F}{2(w_1 + w_2)}\sin((w_1 + w_2)t + \phi_0),$$
$$\gamma \approx \frac{F}{2a(w_1 - w_2)}\cos((w_1 - w_2)t + \phi_0)$$
$$-\frac{F}{2a(w_1 + w_2)}\cos((w_1 + w_2)t + \phi_0).$$

Then, in the spectrum of the variable

$$x = (A_0 + \beta)\sin(w_1 t + \phi_0 + \gamma) \tag{14}$$

one observes the following harmonics: $w_1,\ w_2,\ 2w_1 \pm w_1$. In the case of quadratic coupling

$$Q(x_2, A, \phi) = F(x_2 - x_1)^2 = F(A\sin(w_2 t) - x_1)^2, \tag{15}$$

there appear additional harmonics: $2w_2$, $2w_1$, $2w_1 \pm 2w_2$, $w_1 \pm w_2$, $3w_1 \pm w_2$. In the limit under consideration, with small nonlinearity and weak coupling, the appearance

of these additional combinational harmonics can confidently be associated with the presence of a nonlinear coupling.

It is of course the case that, for a nonlinear oscillator, all sorts of combinational harmonics can in principle appear even for linear coupling. However, the generation of these harmonics is a second order effect which becomes significant only for large nonlinearity and large coupling coefficients. Under the latter circumstances, just the appearance of particular combinational harmonics cannot necessarily be related to a given type of coupling and some further analysis is then required.

References

Bračič M, McClintock P V E and Stefanovska A 2000 Characteristic frequencies of the human blood distribution system in Broomhead D S, Luchinskaya E A, McClintock P V E and Mullin T, eds., *Stochastic and Chaotic Dynamics in the Lakes* (Melville, New York: American Institute of Physics) pp. 146–153

Bračič M and Stefanovska A 1998 Wavelet based analysis of human blood flow dynamics *Bull. Math. Biol.* **60** 919–935

Bračič Lotrič M and Stefanovska A 2000 Synchronization and modulation in the human cardiorespiratory system *Physica A* **283** 451–461

Bračič M and Stefanovska A 1999 Wavelet analysis in studying the dynamics of blood circulation *Nonlinear Phenomena in Complex Syst.* **2** 68–77

Davies L C, Francis D P, Crisafulli A, Concu A, Coats A J S and Piepoli M 2000 Oscillations in stroke volume and cardiac output arising from oscillatory ventilation in humans *Exp. Physiol.* **85** 857–862

Eckberg D L 2003 The human respiratory gate *J Physiol.* **548** 339–352

Fackrell J W A 1996 *Bispectral Analysis of Speech Signals,* PhD thesis, (Edinburgh: University of Edinburgh)

Hales S 1773 *Statistical Essays II, Hæmastatisticks* (London: Innings Manby)

Hinich M J 1982 Testing for Gaussianity and linearity of a stationary time series *J. Time Series Analysis* **3** 169–176

Hinich M J 1990 Detecting a transient signal by bispectral analysis *IEEE Trans. on Acoustics, Speech and Signal Processing* **38** 1277–1283

Hinich M J and Messer H 1995 On the principal domain of the discrete bispectrum of a stationary signal *IEEE Trans. on Signal Processing* **43** 2130–2134

Jamšek J, Stefanovska A, McClintock P V E and Khovanov I A 2003 Time-phase bispectral analysis *Phys. Rev. E* **68** 016201

Kaiser G 1994 *A Friendly Guide to Wavelets* (Boston: Birkhäuser)

Kenner T, Passenhofer H and Schwaberger G 1976 Method for the analysis of the entrainment between heart rate and ventilation rate *Pflügers Archiv.* **363** 263–265

Kuramoto Y 1984 *Chemical Oscillations, Waves, and Turbulence* (Berlin: Springer-Verlag)

Ludwig C 1847 Beiträge zur Kenntniss des Einflusses der Respirationsbewegungen auf den Blatlauf im Aortensysteme *Arch. Anat. Physiol. und Wiss. Med.* **13** 242–302

Nikias C L and Petropulu A P 1993 *Higher-Order Spectra Anlysis: A Nonlinear Signal Processing Framework* (Englewood Cliffs: Prentice-Hall)

Paluš M, Komárek V, Hrnčíř Z and Štěrbová K 2001 Synchronization as adjustment of information rates: Detection from bivariate time series *Phys. Rev. E* **63** 046211

Paluš M and Stefanovska A 2003 Direction of coupling from phases of interacting oscillators: An information-theoretic approach *Phys. Rev. E* **67** 055201(R)

Pflug L A, Ioup G E and Ioup J W 1993 Sampling requirements and aliasing for higher-order correlations *J. Acoust. Soc. Am.* **94** 2159–2172

Pflug L A, Ioup G E and Ioup J W 1994 Sampling requirements for nth-order correlations *J. Acoust. Soc. Am.* **95** 2762–2765

Raschke F 1987 Coordination in the circulatory and respiratory systems in Rensing L, an der Heiden U and Mackey M C, eds., *Temporal Disorder in Human Oscillatory System* (Berlin: Springer) pp. 152–158

Rosenblum M G, Cimponeriu L, Bezerianos A, Patzak A and Mrowka R 2002 Identification of coupling direction: Application to cardiorespiratory interaction *Phys. Rev. E.* **65** 041909

Rosenblum M G and Pikovsky A S 2001 Detecting direction of coupling in interacting oscillators *Phys. Rev. E.* **64** 045202

Rzeczinski S, Janson N B, Balanov A G and McClintock P V E 2002 Regions of cardiorespiratory synchronization in humans under paced respiration *Phys. Rev. E* **66** 051909

Schäfer C, Rosenblum M G, Abel H H and Kurths J 1999 Synchronization in the human cardiorespiratory system *Phys. Rev. E* **60** 857–870

Schäfer C, Rosenblum M G, Kurths J and Abel H H 1998 Heartbeat synchronised with ventilation *Nature* **392** 239–240

Schreiber T 2000 Measuring information transfer *Phys. Rev. Lett.* **85** 461–464

Seidel H and Herzel H 1998 Analysing entrainment of heartbeat and respiration with surrogates *IEEE Eng. Med. Biol. Mag.* **17** 54–57

Sharfer I and Messer H 1993 The bispectrum of sampled data. 1. detection of the sampling jitter *IEEE Trans. on Signal Processing* **41** 296–312

Söderström T, Stefanovska A, Veber M and Svenson H 2003 Involvement of sympathetic nerve activity in skin blood flow oscillations in humans *Am. J. Physiol.: Heart. Circ. Physiol.* **284** H1638–H1646

Stefanovska A 2002 Cardiorespiratory interactions *Nonlinear Phenomena in Complex Systems* **5** 462–469

Stefanovska A and Bračič M 1999 Physics of the human cardiovascular system *Contemporary Physics* **40** 31–55

Stefanovska A, Bračič M and Kvernmo H D 1999 Wavelet analysis of oscillations in the peripheral blood circulation measured by laser Doppler technique *IEEE Trans. Bio. Med. Eng.* **46** 1230–1239

Stefanovska A and Bračič M 1999 Reconstructing cardiovascular dynamics *Control Engineering Practice* **7** 161–172

Stefanovska A, Bračič Lotrič M, Strle S and Haken H 2001a The cardiovascular system as coupled oscillators? *Physiol. Meas.* **22** 535–550

Stefanovska A, Haken H, McClintock P V E, Hožič M, Bajrović F and Ribarič S 2000 Reversible transitions between synchronization states of the cardiorespiratory system *Phys. Rev. Lett.* **85** 4831–4834

Stefanovska A, Luchinsky D G and McClintock P V E 2001b Modelling couplings among the oscillators of the cardiovascular system *Physiol. Meas.* **22** 551–564

van der Pol B and van der Mark J 1928 The heartbeat considered as a relaxation oscillation, and an electrical model of the heart *Philos. Mag.* **7** 763–775

Zhou G and Giannakis G B 1995 Retrieval of self-coupled harmonics *IEEE Trans. on Signal Processing* **43** 1173–1186